

Observations of MSTIDs over South and Central America

C. E. Valladares¹ and R. Sheehan¹

¹Institute for Scientific Research, Boston College

Abstract

TEC values measured by GPS receivers that belong to the low-latitude ionosphere sensor network (LISN) and several other networks that operate in South and Central America were used to study the characteristics and origin of medium-scale traveling ionospheric disturbances (MSTID) in these regions. The TEC perturbations associated with these MSTIDs show a high degree of spatial coherence over distances > 1000 km allowing us to use measurements from receivers spaced by hundreds of km to calculate the MSTID's travel velocities, propagation direction, and scale-size. A pronounced increase in MSTID activity was observed in South and Central America at 16 UT on August 20, 2011 lasting until the end of August 21, 2011. The MSTID velocities show a very variable pattern that depends upon their local time and location. Counter-streaming MSTIDs were observed over the western part of South America on August 21, 2011. Regional maps of tropospheric temperature brightness, measured by the GOES-12 satellite, are used to identify and follow the development of the tropical storm (TS) Irene and several deep convective plumes. MSTIDs were observed propagating away from the TS Irene. This storm moved into the Caribbean region and intensified earlier on August 20 spawning a train of atmospheric gravity waves (AGW). The small scale size, the velocity less than 150 m/s and the close location of several MSTIDs with respect to the TS Irene indicate that these MSTIDs may be the result of primary AGWs that reached the F-region bottomside. These results open the possibility to use TEC values measured by networks of GPS receivers to construct regional, and probably global, maps of MSTIDs, identify their origin and study in detail the characteristics of MSTIDs corresponding to primary and secondary AGWs.

Introduction

Medium-scale traveling ionospheric disturbances (MSTID) consist of ionospheric plasma structures containing horizontal scales sizes of several 100s kms, periods between 15 and 90 min and phase velocities between 100 and 600 m/s [*Hunsucker, 1982*]. At mid latitudes, daytime MSTIDs are regarded as the ionospheric response to atmospheric gravity waves (AGW). Nighttime MSTIDs have a much wider definition including depletions associated with the Perkins instability [*Perkins, 1973*].

Several measuring techniques have been used to study the characteristics and morphology of MSTIDs. Airglow imagers placed at opposite hemispheres have shown the conjugate characteristics of nighttime MSTIDs in the opposite hemisphere [*Otsuka et al., 2004; Shiokawa, et al., 2005, Martinis et al., 2011*]. Radio beacon receivers in the VHF band have shown that daytime and nighttime MSTIDs have different seasonal variations of their occurrence and propagation direction [*Jacobson et al., 1995*]. Similarly, dense networks of GPS receivers have provided 2-D maps of TEC perturbations caused by MSTIDs [*Saito et al., 1998; Afraimovich et al., 2001*].

The modeling study of *Vadas and Liu [2009]* has shown that the dissipation of "primary" GWs can create localized thermospheric body forces able to excite "secondary" large-scale TIDs with a wavelength equal to 2100 km, velocity near 500 m/s and a period of 80 min. *Vadas and Crowley [2010]* have presented evidence that multiple convective plumes can create thermospheric body forces containing smaller scales due to constructive and destructive wave interference. Such body forces are able to excite secondary GWs with smaller horizontal scale sizes.

In the radio beacon technique, also known as radio-interferometry, phase differences measured at the various stations can be used to determine TID velocity, propagation azimuth, and amplitude. Recently, this radio-interferometry technique has been adapted for use with GPS satellites [*Afraimovich, et al. 1998; 2000; 2003*]. This new innovation makes it possible to utilize inexpensive, easily-deployed GPS receivers to study gravity waves at a wide variety of locations.

The main goal of this paper is to describe the results of a method that produces regional maps of TEC perturbations associated with MSTIDs within the South and Central America regions and to relate these observations to maps of tropospheric brightness temperature measured by the GOES-12 satellite. GOES-12 satellite images are used to pinpoint the locations of deep convective plumes across South and Central America and the existence of tropical storms that move throughout the Caribbean region on August 20 and 21, 2011. The paper is organized in the following order: In section 2, we introduce the general characteristics of the cross-correlation analysis that was applied in a regional context to extract the characteristics (e.g. occurrence, velocity, scale size) of the MSTIDs of July 4, 2011. Results of the regional analysis of the TEC observations recorded by hundreds of GPS receivers on August 20 and 21, 2011 are presented in section 3. The association of MSTIDs with tropical storms and convective plumes imaged with the GOES-12 satellite are presented in section 4. The discussion section is presented in sections 5.

2. Analysis of TEC observations for August 20-21, 2011

This section describes the analysis of the MSTIDs that were observed on August 20 and 21, 2011 across South and Central America and the Caribbean region. The goal of this section is to relate the dynamics of the MSTIDs observed on August 20-21, 2011 to the existence of a tropical storm in the Caribbean region and deep convective cells that originated within the central and southern parts of South America.

2.1 Regional maps of MSTIDs occurrence for August 20-21, 2011

The regional maps of Figure 1 show TEC perturbations associated with the MSTIDs that developed over South and Central America on August 20 and 21, 2011. Each frame corresponds to a 4-hour interval in which we have plotted all the MSTIDs detected by the GPS receivers. There was an absence of MSTIDs between 00 and 16 UT on August 20, 2011. After this period, MSTID's population increases across the South American continent in a sector limited between -10° and -20° geographic latitude. The frame, corresponding to the period 20 - 24 UT, displays dTEC perturbations persisting in South America, across the same latitudinal sector observed four hours earlier. This frame also shows MSTIDs extending between the Caribbean Sea and the eastern part of Central America. These newly-developed MSTIDs remain active until 08 UT on the following day. The South American MSTIDs decay before the start of day August 21, 2011. However, they reappear after 15 UT on August 21, 2011. In summary, it was observed that on August 20 and 21, 2011 MSTIDs developed over South America at latitudes slightly south of the magnetic equator between 16 and 24 UT. In fact, during the following 10 days, MSTIDs occur very systematically and almost every day between 16 and 24 UT. In Central America, the Caribbean region and the northern part of South America MSTIDs occur at different time epochs and extending through different areas.

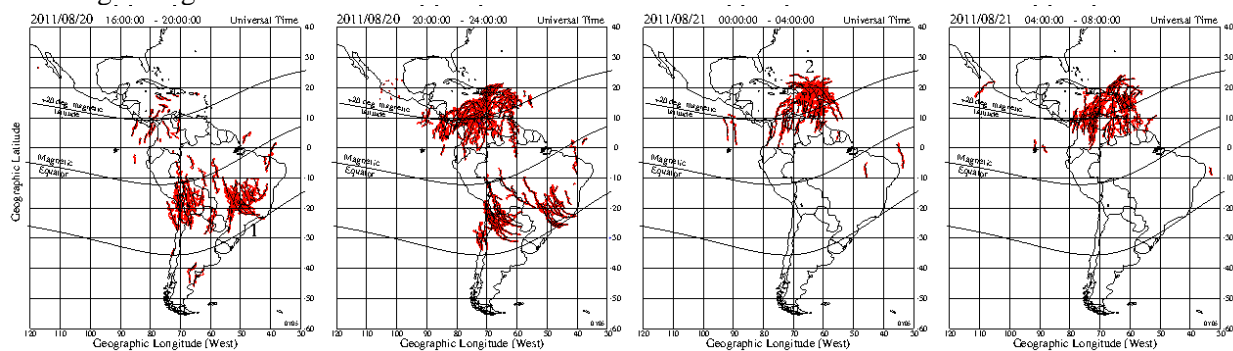


Figure 1. TEC perturbation (TECP) values measured on August 20 and 21, 2011. Each panel displays the amount of MSTIDs observed during a 4-hour segment. Each red segment indicates the amplitude and location of a MSTID detected by our analysis package. Large spaces without red traces are the result of the absence of MSTIDs in those regions.

2.2 Analysis of MSTIDs using a cluster of GPS receivers

Figure 2 displays dTEC perturbations associated with a train of MSTIDs that were detected by one cluster of 11 GPS receivers between 19 and 24 UT on August 20, 2011. These receivers are located in northern Colombia. The dTEC values were derived using signals from the GPS satellite PRN=17. The station's 4-letter name, the latitude and the longitude are indicated in the right margin. Note also that the amplitude of the dTEC is printed at the middle right side and it is equal to 5 TEC units. From top to bottom the stations are organized following their geographic latitude, starting at the top with the station placed further north, Santa Marta (Isam) and ending with Bogota (lbo_). These two stations belong to the LISN network. This display arrangement helps us to discern the propagation direction of the MSTID. We select a conspicuous feature within the dTEC traces, like the largest minimum or maximum, and determine how this feature time shifts at different sites. Red arrows indicate the time when the largest minimum occurs for each of the eleven traces of Figure 2. As this feature appears at earlier times at sites that are placed further south, it is concluded that the MSTIDs observed on August 20, 2011 in northern Colombia are propagating northward. We also calculate the average period of the MSTIDs equal to 63 min and the spectrum bandwidth 44 min. We also indicate that some of the stations present rapid dTEC fluctuations, as seen at Dorada (dora) and Aguachica (agua) at 22 UT. This effect is likely produced by the transit of additional MSTIDs containing shorter spatial scales.

Figures 3 shows the velocity analysis for 3 stations (Corozal, Cucuta and Maracaibo) that are part of the cluster of GPS receivers presented in Figure 2. To avoid contamination produced by MSTIDs that have periods different than 63 min and are transiting across the stations with different velocities and scale sizes, we apply a band-pass filter to the dTEC traces and filtered out these unwanted MSTIDs. The middle frames display the dTEC traces after they have been filtered using a band-pass filter centered at 63 min (0.2 mHz). The top panels display the cross-correlation functions (CCF) in which two peaks separated by ~ 60 min are evident produced by the periodicity of the MSTIDs. To determine the peak associated with the true motion of the MSTIDs, we use the information provided by Figure 2 in which it was realized that the MSTIDs were moving northward. Note that a negative (positive) offset is an indication that Corozal's TEC perturbation lags (leads) Cucuta's. As Corozal is located north of Cucuta and south of Maracaibo, to calculate the MSTID's velocity we considered the CCF peak with a negative delay for the first pair of stations (Corozal and Cucuta) and the positive delay for the second pair (Corozal and Maracaibo). Similar analysis was performed for every set of 3 different receivers of the cluster of GPSs depicted in Figure 2.

The velocity of the train of MSTIDs is shown in the lower panel of Figure 3. This velocity is equal to 250 m/s and directed northward at 20 UT, and becomes northwestward at 24 UT. These values confirm the direction of motion that was determined based on the time-shift of the largest minimum of Figure 2; at the same time they provide a more precise estimate of the MSTID transit motion. It is indicated that similar

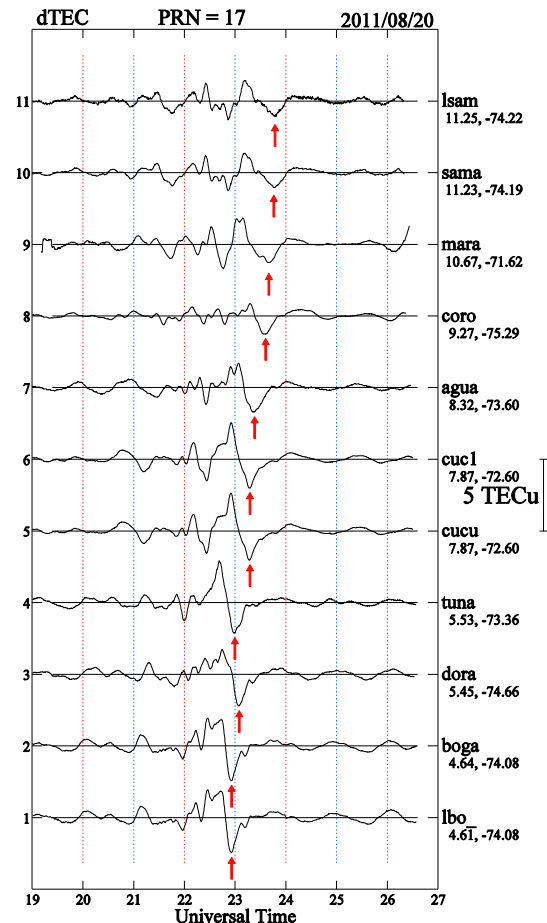


Figure 2. dTEC values measured by 11 stations located in northern Colombia and Venezuela. The red arrows indicate the time when the minimum dTEC value was found in each trace.

phase velocities were determined when our analysis procedure was performed using other receivers that belong to the GPS cluster of Figure 2.

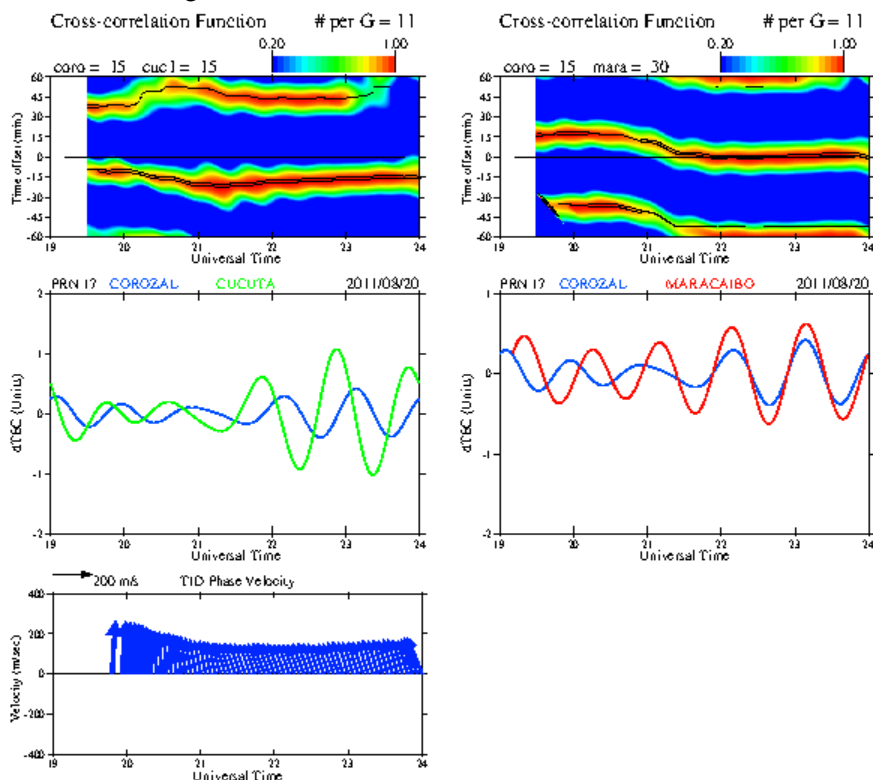


Figure 3. Cross correlation functions (top panels) and TECP curves (lower frames) for GPS satellite 17 and stations Corozal and Cucuta in the left frames and Corozal and Maracaibo in the right frames. The lower panel shows the phase velocities of the MSTIDs calculated using the time delays provided by the CCM algorithm (upper frames).

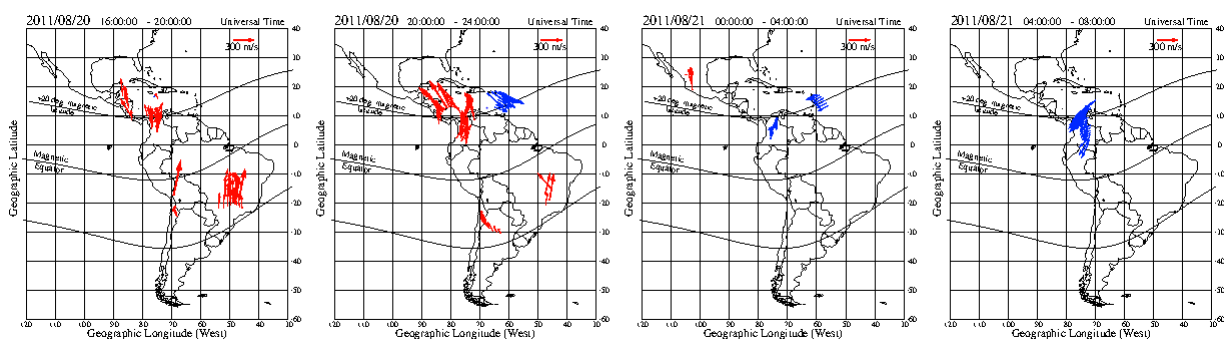


Figure 4. MSTID's phase velocities calculated using the CCM algorithm. Red arrows are used for velocities having a northward component. Blue arrows correspond to velocities that have a southward component.

2.3 Regional maps of MSTIDs velocity for August 20-21, 2011

Figure 4 compiles the MSTID's velocity information from the majority of the GPS clusters. Red vectors indicate northward velocities and blue vectors depict velocities with a southward component. The velocity field was decimated a factor of 8 to avoid cluttering the figure. The main characteristic of the plots is the general trend of the velocities: they are principally directed northward or southward. Although, there exist some exceptions and the MSTID velocity can have a small westward or eastward

component during the early evening and early hours of the day. On August 20, 2011 at 16 UT, the velocities over South America vary between 200 - 500 m/s. At this time the MSTID's velocities are mainly directed northward with a $\pm 20^\circ$ directional variability. The following frame corresponding to 20-24 UT shows the velocities directed northwestward in the northern part of South America. These velocities intrude into Central America reaching values as high as 400 m/s. There also exists a region near Puerto Rico, where velocities are directed southeastward reaching 420 m/s.

The next frame, corresponding to August 21, 2011 at 00-04 UT, displays velocities over the eastern side of the Caribbean region, where the flow is ~ 200 m/s and it is directed southwestward. Downstream in eastern Colombia, the MSTID's velocities were also pointing southwestward, but the velocity magnitude was ~ 300 m/s.

3. GOES-12 Infrared images

The Geostationary Satellite system (GOES) mission provides weather monitoring and forecasting operations, and aids research to understand land, atmosphere, ocean, and climate interactions. GOES-12 was launched in 2001, and has been in standby orbit most of its lifetime. However, during a few months in 2011, GOES-12 operated in the GOES-EAST position, providing coverage of the east coast of the United States and South America. The spacecraft was designed to "stare" at the earth and image clouds, monitor earth's surface temperature and water vapor fields, and sound the atmosphere for its vertical thermal and vapor structures.

The imager on board GOES-12 is a multichannel instrument that senses infrared radiant energy and visible reflected solar energy from the Earth's surface and atmosphere. The satellite also measures the temperature of the clouds and the surface of the Earth with an infrared sensor. This allows for the detection of changes in the temperature of clouds during the day and at night. The temperature of the clouds also indicates how tall clouds are since temperature is inversely proportional to height in the atmosphere. Red color indicates the appearance of temperatures as cold as -80° C and clouds extending up to 11,000-12,000 meters. *Vadas and Crowley [2010]* pointed out that the type of clouds that prevail in Central and South America consist of convective plumes able to trigger gravity waves that propagate through the troposphere and mesosphere, which dissipate in the thermosphere (or mesosphere) and create body forces that are able to generate secondary gravity waves that can reach F-region altitudes.

Figure 5 shows an image taken with the infrared sensor on-board GOES 12 on August 20, 2011 at 23:45 UT. Several series of convective plumes were seen within Central and South America during two days when tropical storm Irene developed in the Caribbean region (see storm north of Venezuela). This frame, corresponding to 23:45 UT on August 20, 2011, shows the remnants of a tropical depression that originated over the Pacific Ocean, drifted northeast, and was located over Central America at the time of the GOES-12 image. Figure 9 also displays the formation of a tropical depression moving north of the northern coast of South America (yellow arrow). A few hours later this tropical depression became organized enough to be classified as tropical storm Irene.

4. Discussions

When primary AGWs are created near the tropopause, they travel outward from the origin in all directions forming at mesospheric altitudes an almost circular pattern of perturbed densities. At higher

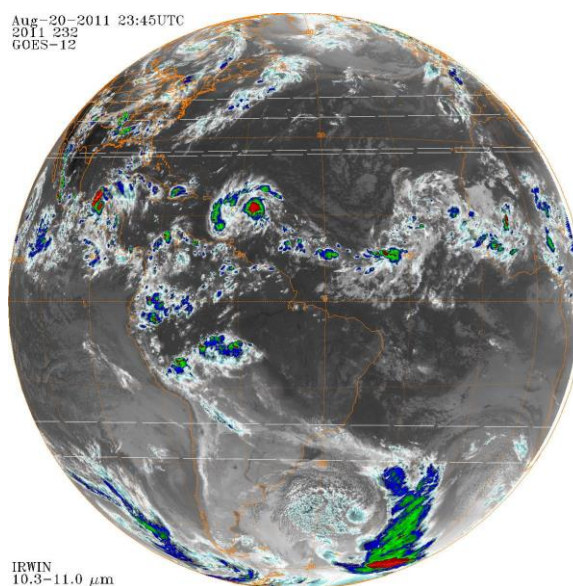


Figure 5. Image observed with the GOES 12 satellite corresponding to August 21, 2011, 00:00 UT.

altitudes, the variable thermospheric wind filters the AGWs in some directions leaving a segmented pattern of AGWs propagating only at selected directions. Saturation, wind filtering and wave breaking make the primary waves dissipate and transfer momentum to the atmosphere creating horizontal body forces [Vadas and Fritts, 2004]. AGWs containing large scale sizes might be able to propagate to the F-region bottomsides. Smaller scale AGWs (20 – 30 km) dissipate at 90 km and others with larger sizes (50 – 150 km) at 140 km, creating mesospheric and thermospheric body forces respectively [Vadas and Crowley, 2010]. These body forces excite large-scale, upward and downward propagating secondary AGWs and then TIDs with scale sizes between 1000 and 2000 km, horizontal velocity ~ 500 m/s and periods ~ 80 min which propagate away from the body forces, traveling up to altitudes as high as 400 km [Vadas and Liu, 2009]. AGWs propagating against the neutral wind can reach the F-region bottomsides and produce MSTIDs by moving plasma along the magnetic field lines [Hines and Reddy, 1967; Fritts and Vadas, 2008].

However, AGWs propagating in the same direction of the neutral wind dissipate due to the wind filtering effect.

Figure 6 shows precipitation rainfall measured by the Tropical Rainfall Measuring Mission (TRMM) satellite on August 21, 2011 at 00 UT. TRMM is a joint US-Japan satellite mission to monitor tropical and subtropical precipitation and to estimate its associated latent heat. Figure 6 displays (1) the amount of rainfall in mm/hour in the American sector, (2) black arrows representing neutral wind vectors from the Hedin Wind model (HWM) at 200 km altitude [Hedin *et al.*, 1988], and (3) TEC perturbations (in purple). Note that the TECs and the rain associated with TS Irene are contained inside a yellow circle. Figure 6 points out that the neutral wind velocity over the Caribbean region, where TS Irene developed is ~ 100 m/s directed eastward. This magnitude and direction of the wind make waves propagating eastward to dissipate. However, it favors the propagation of AGWs in the opposite direction as seen in Figure 4.

5. Conclusions

This study has led to the following:

1. This analysis has provided regional maps of TEC perturbations associated with the MSTIDs that circulated throughout South and Central America and the Caribbean region on August 20 and 21, 2011. Similar plots can be constructed for other continents such as Africa and Asia to further our understanding on the longitudinal differences that exist in different regions of the Globe.
2. Calculations of the phase velocity and the scale size of MSTIDs and regional images of tropospheric temperature brightness recorded by the GOES-12 satellite were used to assess the role of a tropical storm and clusters of tropospheric convective cells on the initiation of MSTIDs in the South America continent.
3. A group of MSTIDs, observed in the Caribbean region between 0 and 06 UT on August 21, 2011,

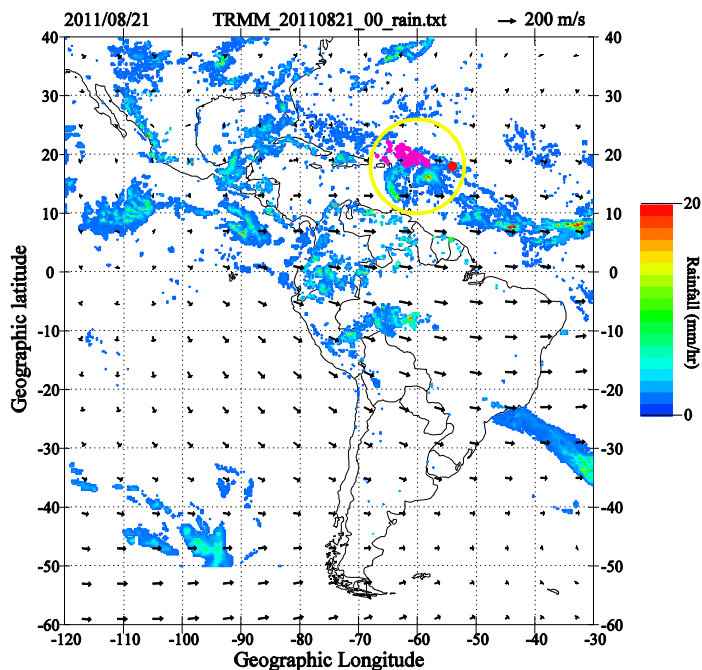


Figure 6. Rainfall measured by the TRMM satellite over South and Central America and the Caribbean region on August 21, 2011 at 00 UT. Note the region of heavy rain at the location of the tropical storm Irene. The positive values of dTEC, displayed in Figure 1, are displayed in purple.

were likely associated with primary AGWs. These waves were triggered within the region of TS Irene. These MSTIDs were moving eastward at 140 m/s and had a scales size of 250 km.

References

- Afraimovich, E. L., et al. (1998), GPS radio interferometry of travelling ionospheric disturbances, *J Atmos Sol-Terr Phy*, 60, 1205-1223.
- Afraimovich, E. L., Kosogorov, E. A., Perevalova, N. P., & Plotnikov, A. V. (2001). The use of GPS arrays in detecting shock-acoustic waves generated during rocket launchings. *Journal of Atmospheric and Solar-Terrestrial Physics*, 63(18), 1941–1957.
- Fritts, D. C., and S. L. Vadas (2008), Gravity wave penetration in to the thermosphere: Sensitivity to solar cycle variations and mean winds, *Ann. Geophys.*, 26, 3841–3861.
- Hines, C. O., and C. A. Reddy (1967), On the propagation of atmospheric gravity waves through regions of wind shear, *J. Geophys. Res.*, 72, 1015–1034.
- Hocke, K., and T. Tsuda (2001), Gravity waves and ionospheric irregularities over tropical convection zones observed by GPS/MET radio occultation, *Geophys. Res. Lett.*, 28, 2815–2818.
- Hunsucker, R. D. (1982), Atmospheric gravity waves generated in the high-latitude ionosphere: A review, *Rev. Geophys.*, 20(2), 293–315, doi:[10.1029/RG020i002p00293](https://doi.org/10.1029/RG020i002p00293).
- Martinis, C., J. Baumgardner, J. Wroten, and M. Mendillo (2011), All-sky imaging observations of conjugate medium-scale traveling ionospheric disturbances in the American sector, *J. Geophys. Res.*, 116, A05326, doi:[10.1029/2010JA016264](https://doi.org/10.1029/2010JA016264).
- Otsuka, Y., K. Shiokawa, T. Ogawa, and P. Wilkinson (2004), Geomagnetic conjugate observations of medium-scale traveling ionospheric disturbances at midlatitude using all-sky airglow imagers, *Geophys. Res. Lett.*, 31, L15803, doi:[10.1029/2004GL020262](https://doi.org/10.1029/2004GL020262).
- Perkins, F. (1973), Spread *F* and ionospheric currents, *J. Geophys. Res.*, 78(1), 218–226, doi:[10.1029/JA078i001p00218](https://doi.org/10.1029/JA078i001p00218).
- Saito, A., T. Iyemori, and M. Takeda (1998), Evolutionary process of 10 kilometer scale irregularities in the nighttime midlatitude ionosphere, *J. Geophys. Res.*, 103(A3), 3993–4000.
- Shiokawa, K., et al. (2005), Geomagnetic conjugate observation of nighttime medium-scale and large-scale traveling ionospheric disturbances: FRONT3 campaign, *J. Geophys. Res.*, 110, A05303, doi:[10.1029/2004JA010845](https://doi.org/10.1029/2004JA010845).
- Vadas, S. L., and D. C. Fritts (2004), Thermospheric responses to gravity waves arising from mesoscale convective complexes, *J. Atmos. Sol. Terr. Phys.*, 66, 781–804.
- Vadas, S.L., and H. Liu (2009), Generation of large-scale gravity waves and neutral winds in the thermosphere from the dissipation of convectively generated gravity waves, *J. Geophys. Res.*, 114, A10310, doi:[10.1029/2009JA014108](https://doi.org/10.1029/2009JA014108).
- Vadas, S. L. and G. Crowley (2010), Sources of the traveling ionospheric disturbances observed by the ionospheric TIDBIT sounder near Wallops Island on October 30, 2007, *J. Geophys. Res.*, 115, A07324, doi:[10.1029/2009JA015053](https://doi.org/10.1029/2009JA015053).
- Valladares C. E., and M. A. Hei (2011), Measurement of the characteristics of TIDs using three GPS receivers at Huancayo, Peru, submitted to *J. Atmos. and Solar-Terr. Phys.*